



Electrochemical pitting behaviour of type 321 stainless steel in sulfide-containing chloride solutions

Y.M. LIOU, S.Y. CHIU, C.L. LEE and H.C. SHIH*

Department of Material Science and Engineering, National Tsing Hua University, Hsinchu, Taiwan 300, Republic of China

(*author for correspondence, e-mail: hcshih@mse.nthu.edu.tw)

Received 16 December 1998; accepted in revised form 27 April 1999

Key words: cyclic potentiodynamic polarization, pitting, sodium chloride, sodium thiosulfate, type 321 stainless steel

Abstract

The pitting behaviour of type 321 stainless steel in sulfide-containing chloride aqueous environments was studied using cyclic potentiodynamic polarization. A well-established correlation between H_2S and $\text{Na}_2\text{S}_2\text{O}_3$ in the study of corrosion was applied, that is, H_2S was simulated by $\text{Na}_2\text{S}_2\text{O}_3$. The major factors affecting the pitting corrosion of type 321 stainless steel are the Cl^- concentration, solution pH and temperature. The results clearly indicate that both E_{pit} and E_{pp} decrease with increasing Cl^- concentration and temperature, while I_{pass} is more sensitive to temperature variation. E_{pit} decreased with decreasing pH in the range $2 < \text{pH} < 7.5$. The surface morphology and chemistry of the corroded type 321 stainless steel resulting from anodic polarization in $0.01 \text{ M S}_2\text{O}_3^{2-}$ -containing Cl^- solution were analysed by XRD, SEM and EPMA. A higher concentration of sulfur was found in the pits, and the dark surface film was mainly composed of FeS and $\gamma\text{-Fe}_2\text{O}_3$. The results describe the pitting behaviour of type 321 stainless steel in sulfide-containing Cl^- aqueous environments.

1. Introduction

Corrosion has always been a problem in petroleum refining and petrochemical operations. Uniform corrosion of equipment can be readily detected by various inspection techniques. In contrast, isolated pitting is potentially much more serious because leakage can occur at highly localized areas that are difficult to detect [1–3]. Stainless steels (SS) are extensively used in petrochemical refineries, because of the highly corrosive nature of the catalysts and solvents that are often used [3]. Most stainless steels will pit in the presence of chlorides. Hydrogen sulfide is the main constituent of refinery sour waters and is also formed by the decomposition of organic sulfur compounds that are present at elevated temperatures [4–6]. The type 321 SS used in this study was a titanium-stabilized austenitic stainless steel. Sensitization resulting from the precipitation of chromium carbide along the grain boundaries is avoided by alloying titanium with the native carbon in the form of TiC precipitates at much higher temperatures. The use of H_2S in this study was replaced by $\text{Na}_2\text{S}_2\text{O}_3$, the latter being more convenient and less hazardous to the environment. A series of simple immersion tests in deaerated 20 wt % NaCl solution at 80°C indicated a good correlation between the critical pitting concentration of $\text{S}_2\text{O}_3^{2-}$

and the critical H_2S pressure for pitting [7], leading to a standard simulated $\text{Cl}^- + \text{H}_2\text{S}$ environment being proposed [8, 9] consisting of deaerated 20 wt % $\text{NaCl} + 10^{-3}\text{--}10^{-2} \text{ M S}_2\text{O}_3^{2-}$ aqueous solution of pH 4 at 80°C . However, in the present work a more acidified environment of pH 2 was also adopted in the polarization tests of type 321 SS.

By means of the cyclic potentiodynamic polarization [10], the effects of Cl^- concentration, temperature, and solution pH on the pitting corrosion behaviour of type 321 SS in sulfide-containing Cl^- environments were investigated.

2. Experimental details

2.1. Materials

Coupons of type 321 SS were cut from commercial stock, fully annealed, abraded with a series of SiC papers to 600 grit, followed by ultrasonic cleaning in acetone and finally rinsing in deionized water prior to the immersion tests. The specimen area exposed to the test solution was 1 cm^2 and the remaining area was shielded by epoxy resin. The chemical compositions (wt %) analysed by atomic emission spectroscopy were: 0.069 C, 1.30 Mn, 0.023 P, 0.006 S,

0.60 Si, 10.96 Ni, 17.89 Cr, 0.50 Ti, 0.86 Mo and balanced Fe.

2.2. Cyclic potentiodynamic polarization

The polarization apparatus was similar to the standard assembly as described elsewhere [11–13]. A standard calomel electrode (SCE) and a graphite electrode were used as reference and counter electrode, respectively and an EG&G model 273 potentiostat/galvanostat for the polarization of the specimen. Figure 1 shows a schematic of the cyclic polarization curve for a metal that pits. A scan rate of 1 mV s^{-1} was found convenient and sufficiently slow to avoid any loss of configuration of the potentiodynamic polarization curves. All specimens were initially polarized from their natural corrosion potential, designated as E_{corr} and subsequently controlled cathodically at -1.2 V vs SCE, a potential which is significantly below E_{corr} , for about 10 min to reduce the possible existing surface films, then reversed to where the polarization started. A new potential E_c was found to be more active than E_{corr} . The second reverse occurred at potentials significantly more noble than E_{corr} or at the current density $>10^{-3} \text{ A cm}^{-2}$. The potential was then swept to more active values and the cyclic polarization was thus completed.

2.3. Test solution

The test solutions were prepared with deionized water and reagent-grade NaCl, and $\text{Na}_2\text{S}_2\text{O}_3 \cdot 5\text{H}_2\text{O}$. The solution pH was adjusted by either adding HCl or NaOH. Deaeration of the test solution was achieved by purging the solution with deoxygenated nitrogen for 1 h

prior to the test and continuing the purging during the test.

3. Results and discussion

3.1. Effect of Cl^- concentration

The effects of Cl^- concentration on the potentiodynamic polarization curve of type 321 SS in deaerated $0.01 \text{ M S}_2\text{O}_3^{2-}$ -containing Cl^- aqueous solution (pH 7) at 25°C are shown in Figure 2(a) and (b). The curves indicate that: (i) increasing Cl^- concentration shifts both the pitting potential (E_{pit}) and the protection potential (E_{pp}) in the active direction; Cl^- exerts a noticeable influence on the pitting susceptibility; (ii) linear relationships between E_{pit} and E_{pp} as functions of Cl^- concentration were observed [14–16], these are: $E_{\text{pit}}(v) = -0.110 - 0.153 \log [\text{Cl}^- \text{ wt \%}]$ and $E_{\text{pp}}(v) = -0.252 - 0.136 \log [\text{Cl}^- \text{ wt \%}]$, respectively, indicating that E_{pit} and E_{pp} are highly susceptible to Cl^- concentration, while the difference between E_{pit} and E_{pp} , that is, ΔE remains

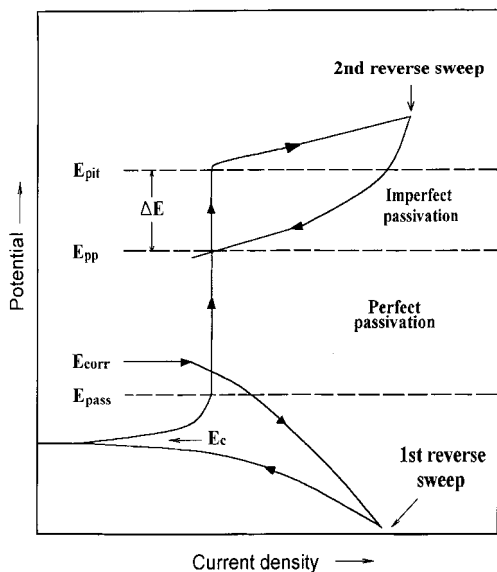


Fig. 1. Schematic of cyclic polarization curve for a metal that pits.

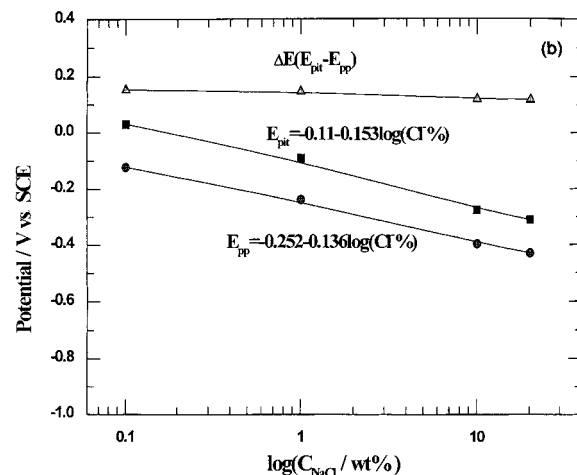
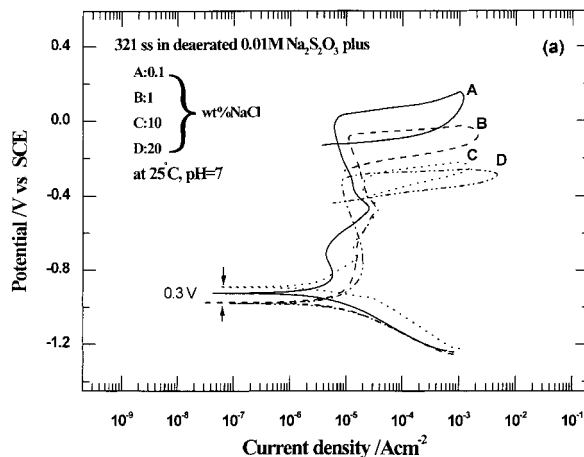


Fig. 2. Effect of Cl^- concentration on the polarization behaviour of type 321 SS in deaerated $0.01 \text{ M S}_2\text{O}_3^{2-}$ -containing Cl^- aqueous solutions at pH 7 and 25°C , (a) anodic polarization curves for Cl^- (wt %) of 0.1, 1, 10, and 20, and (b) variation of E_{pit} , E_{pp} , and ΔE with the Cl^- concentration.

constant. The magnitude of ΔE was often considered as an indicator for pitting resistance; that is, the smaller the ΔE , the higher the pitting resistance [14, 17]. However, the difference between E_{corr} and E_{pp} has been considered as a critical indication of pitting resistance in recent years. E_{corr} changes only slightly with Cl^- concentration within 0.3 V (Figure 2(a)) and lies much below the E_{pp} by 0.73 to 0.45 V as Cl^- concentration increases from 0.1 wt % to 20 wt % where type 321 SS is entirely free from pitting corrosion.

3.2. Effect of temperature

Temperature increases the rate of almost all chemical reactions. It is vital in this particular environment containing $\text{S}_2\text{O}_3^{2-}$. Figure 3 shows the potentiodynamic polarization results of type 321 SS in a deaerated 0.01 M $\text{S}_2\text{O}_3^{2-}$ -containing Cl^- solution (pH 7) at temperatures 30–92 °C. It is clear that both E_{pit} and E_{pp} decrease with increasing temperature. It is worth noting that E_{corr} shifts slightly in the noble direction with increasing

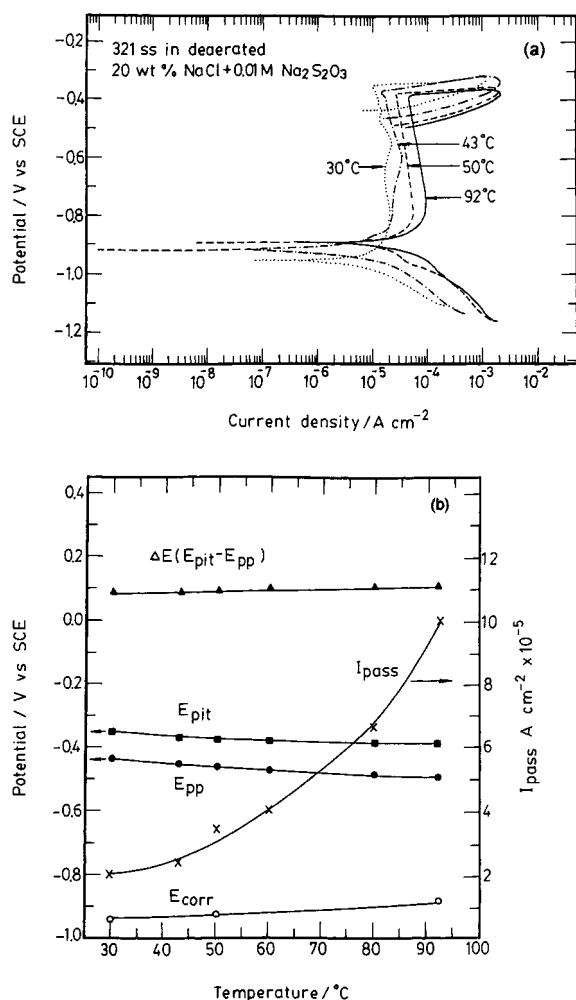


Fig. 3. Effect of temperature on the anodic polarizations of type 321 SS in 0.01 M $\text{S}_2\text{O}_3^{2-}$ -containing 20 wt % Cl^- aqueous solution at pH 7 and 25 °C, (a) polarization curves taken at different temperatures, and (b) variation of E_{pit} , E_{pp} , E_{corr} , ΔE and I_{pass} with the temperature.

temperature, which suggests that depolarization of the cathodic reaction takes place, resulting in a higher corrosion rate while the polarization of the anodic reaction remains constant. The passive current density I_{pass} increases from 2×10^{-5} to $10 \times 10^{-5} \text{ A cm}^{-2}$ as the temperature is varied from 30 to 92 °C (Figure 3(a) and (b)). Increasing temperature apparently promotes the ionic activities of Cl^- and $\text{S}_2\text{O}_3^{2-}$ and a possible synergistic effect causes breakdown of the passive film and reduces pitting resistance.

3.3. Effect of solution pH-corrosion behaviour diagram

Various characteristic potentials, such as E_{corr} , E_c , E_{pp} and E_{pit} , derived from the cyclic potentiodynamic polarizations for type 321 SS in deaerated 0.01 M $\text{S}_2\text{O}_3^{2-}$ -containing Cl^- aqueous solutions expressed as a function of solution pH, also known as the corrosion behaviour diagram, was constructed, as shown in Figure 4. It is apparent that E_{pit} decreases with decreasing solution pH, thereby reducing the resistance for pitting, while $\Delta E (E_{\text{pit}} - E_{\text{pp}})$ which covers the region of imperfect passivation increases linearly with pH in the range pH 2 to 7.5. The extent of the perfect passivation region starts to reduce more significantly in solution of pH < 4. The pH 1.9 line divides the diagram into areas of general corrosion and passivation. This boundary was carefully determined by polarizing the specimen anodically using small pH increments, and noting a transition from the active state of general corrosion to the passive state [10, 18, 19]. The type 321 SS used in this study remains passive to pH values as low as 1.9, compared with 8.2 for mild steel in a similar environment [10]. The pH-varying E_{corr} lies along the boundary of E_{pp} and intersect it at pH 4, or more quantitatively, $E_{\text{corr}} > E_{\text{pp}}$ at pH ≤ 4 where type 321 SS suffers from pitting corrosion; on the other hand, $E_{\text{corr}} < E_{\text{pp}}$ at pH ≥ 4 where type 321 SS is entirely immune from any type of corrosion (Figure 4). E_{corr} specifies the potential of a metal that exhibits passivity in most air-saturated solutions. For instance, chromium, although

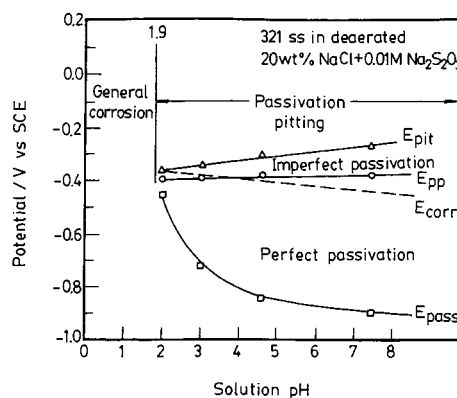


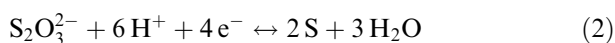
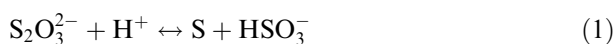
Fig. 4. Corrosion behaviour diagram for type 321 SS in deaerated 0.01 M $\text{S}_2\text{O}_3^{2-}$ -containing 20 wt % Cl^- aqueous environment with varying solution pH values at 25 °C.

near zinc ($E^\circ = -0.763$ V) in the electromotive series, behaves more like silver ($E^\circ = 0.799$ V) in many air-saturated aqueous solutions because of its passive surface film. Chromium and stainless steels can even be passivated in air. Pitting was observed at $1.9 < \text{pH} \leq 4$, while no pitting occurred for $\text{pH} > 4$. This observation is summarized in the corrosion behaviour diagram of Figure 4 as derived from anodic polarization curves. For $\text{pH} \sim 2$ where curves of E_{corr} and E_{pit} meet, pits developed almost instantaneously, whereas for $\text{pH} < 1.9$, pitting corrosion could be considered as totally masked by general corrosion. The region below E_{pass} also suffers from general corrosion and is not a major concern, since E_{corr} is more noble than these potentials, especially for $\text{pH} > 4$ where passivity remains intact. The passive current density, I_{pass} increases slightly with decreasing pH in the pH range 7.5 to 2, showing that the protective ability of the passive oxide film becomes weaker and less corrosion-resistant in acid solutions.

3.4. Pit morphology and corrosion product

Either colloid formation or lower metal overvoltage resulting from the chemisorption of Cl^- ions under anodic polarization may cause local breakdown of the passive film. The appearance of pits, in which sulfur is deposited in a solution pH 2, is shown in Figure 5(a) and (b), while the alloying element Ti (0.5%) for the stabilizing does not show any localized enrichment, as shown in Figure 5(c). However, when uniform corrosion takes place for $\text{pH} < 1.9$, only a dark layer of FeS, along with $\gamma\text{-Fe}_2\text{O}_3$, was detected by XRD as shown in Figure 6. Both S and H_2S originate from $\text{S}_2\text{O}_3^{2-}$ as a result of the following chemical and electrochemical decompositions [1, 7, 20, 21].

Formation of S:



Formation of H_2S :



These reactions can be further enhanced by increasing temperature and/or acidity of the environments.

The resulting FeS film is also confirmed by the potential-pH diagram for Fe-S-H₂O [22] where a constant pH line occurs at $\text{pH} \sim 2$ where FeS and $\text{Fe}^{2+} + \text{H}_2\text{S}$ are in electrochemical equilibrium. For $\text{pH} > 2$ FeS is a stable phase from -0.15 to -0.65 V vs SCE, which corresponds to the areas of pitting, imperfect passivation, perfect passivation, and the complete distribution of E_{corr} , as observed in the corrosion behaviour diagram (Figure 4).

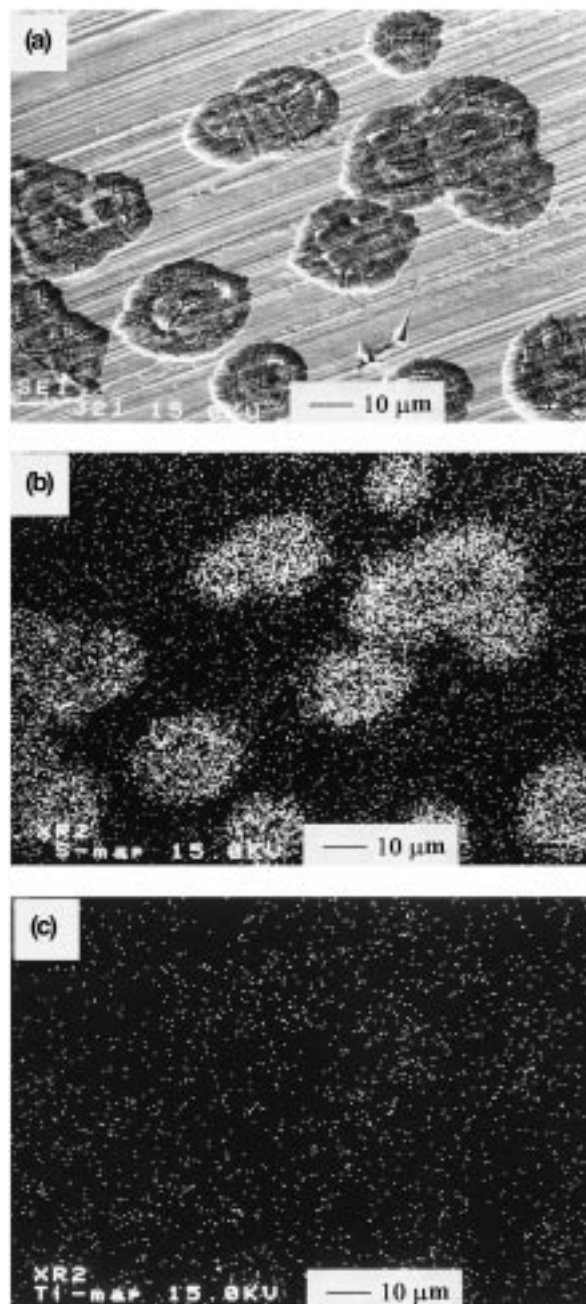


Fig. 5. Photomicrograph and element distribution of type 321 SS in deaerated 0.01 M $\text{S}_2\text{O}_3^{2-}$ -containing 20 wt % Cl^- aqueous solution at pH 2 and 25 °C, (a) SEM micrograph, (b) X-ray mapping of sulfur and (c) X-ray mapping of titanium.

4. Conclusions

The following conclusions can be drawn:

- (i) Increasing Cl^- concentration in the presence of 0.01 M $\text{Na}_2\text{S}_2\text{O}_3$ decreases E_{pit} and E_{pp} with the following relations: $E_{\text{pit}}(v) = -0.110 - 0.153 \log [\text{Cl}^- \text{ wt } \%]$ and $E_{\text{pp}}(v) = -0.252 - 0.136 \log [\text{Cl}^- \text{ wt } \%]$. Both E_{pit} and E_{pp} are highly susceptible to the Cl^- concentration, while the ΔE or $E_{\text{pit}} - E_{\text{pp}}$ remains constant at about 180 mV and is almost independent of Cl^- concentration.

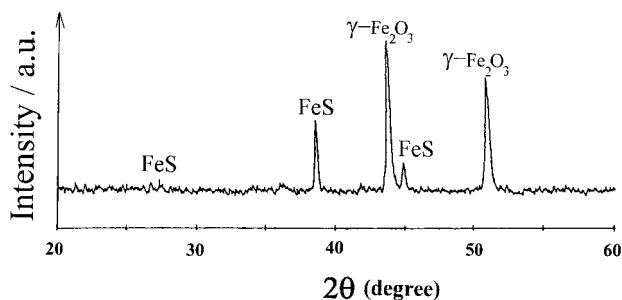


Fig. 6. X-ray diffraction pattern of type 321 SS after anodic polarization in deaerated 0.01 M $S_2O_3^{2-}$ -containing 20 wt % Cl^- aqueous solution at pH 2 and 25 °C, showing the major corrosion product of FeS along with γ - Fe_2O_3 .

- (ii) Both E_{pit} and E_{pp} decrease with increase in temperature, accounting for the increase in ionic activity of Cl^- and $S_2O_3^{2-}$ or, more precisely, their synergism effects, which promote passivity breakdown. I_{pass} increases with increasing temperature.
- (iii) E_{pit} decreases with increasing acidity of $S_2O_3^{2-}$ -containing Cl^- solutions and therefore increases the tendency for pitting. The perfect passivation region shrinks rapidly as E_{pass} rises cathodically (more noble potentials) in solutions of pH < 4. The superimposed E_{corr} distribution intersects E_{pp} , which is the boundary between imperfect passivation and perfect passivation at pH 4. Type 321 SS is extremely susceptible to pitting corrosion in the range $2 < pH < 4$. It is apparently safe to use type 321 SS in similar environments but of higher pH, that is pH > 5.
- (iv) Sulfur was the only chemical residue observed in the pits ($2 < pH < 4$), while FeS, along with γ - Fe_2O_3 , was detected as the major chemical components of the surface film resulting from general corrosion (pH < 1.9).

Acknowledgements

The authors gratefully acknowledge financial support from the Chinese Petroleum Corporation and also from the National Science Council of the Republic of China under contract NSC 85-2216-E-007-012.

References

1. R.D. Kane, *Int. Metals Rev.* **30** (1985) 291.
2. H.I. McHenry, P.T. Purtscher and T.R. Shives, *Corros. Sci.* **27** (1987) 1041.
3. R.D. Merrick, *Mater. Perform.* **27** (1988) 30.
4. Z.A. Foroulis, *Corros. Prevent. Control* **40** (1993) 84.
5. G.E. Moller, I.A. Franson and T.J. Nichol, *Mater. Perform.*, Vol 20 (No. 4), 1981, p 41–50.
6. J. Gutzeit, R.D. Merrick and L.R. Scharfstein, 'Corrosion in Petroleum Refining and Petrochemical Operations, Metals Handbook', Vol. 13, Corrosion, 9th edn. (ASM International, Metals Park, OH, 1987), p.1262.
7. NACE Standard TM 01-77, 'Laboratory Testing of Metals for Resistance to Sulfide Stress Cracking in H_2S Environment' (NACE, Houston, TX, 1990).
8. S. Tsujikawa, A. Miyasaka, M. Ueda, S. Ando, T. Shibata, T. Haruna, M. Katahira, Y. Yamane, T. Aoki and T. Yamada, *Corrosion* **49** (1993) 409.
9. T. Haruna and T. Shibata, *Corrosion* **50** (1994) 785.
10. H.C. Shih, J.C. Oung, J.T. Hsu, J.Y. Wu and F.I. Wei, *Mater. Chem. Phys.* **37** (1994) 230.
11. N.D. Greene, 'Experimental Electrode Kinetics' (Rensselaer Polytechnic Institute, Troy, NY, 1965).
12. G.A. Cragolino and N. Dridhar, *Corrosion* **25** (1969) 233.
13. M. Hubbell, C. Price and R. Heidersbach, 'Crevice and pitting corrosion test for stainless steels', in 'Laboratory Corrosion Tests and Standards' (edited by G.S. Haynes and R. Baboian) (ASTM STP 886, 1985), p. 324.
14. B.E. Wilde, *Corrosion* **28** (1972) 283.
15. T. Suzuki and Y. Kitamura, *Corrosion* **28** (1972) 1.
16. D.A. Jones and B.E. Wilde, *Corros. Sci.* **18** (1978) 631.
17. H.P. Leckie and H.H. Uhlig, *J. Electrochem. Soc.* **113** (1966) 1262.
18. S.D. Chyou and H.C. Shih, *Bull. Electrochem.* **3** (1987) 1.
19. S.D. Chyou and H.C. Shih, *Corrosion* **47** (1991) 31.
20. A.M. Pedraza, I. Villegas, B. Chornik and P.L. Freund, *J. Electroanal. Chem.* **250** (1988) 443.
21. G. Schmitt, *Corrosion* **471** (1991) 288.
22. R.C. Newman, K. Sieradzki and H. S. Isascs, *Metall. Trans. A* **13** (1982) 2015.